Mathematical Model for the Prediction of Gas–Liquid Mass Transfer in Airlift Contactors

P. Pavasant
P. Wongsuchoto
V. Suksoir
Department of Chemical Engineering
Faculty of Engineering
Chulalongkorn University, Bangkok 10330 THAILAND
Email: prasert.p@chula.ac.th

A mathematical model was proposed to explain the gas–liquid mass transfer behavior in an airlift contactor (ALC). The model separated the airlift contactor into three sections: riser, gas separator, and downcomer. The riser and downcomer were described using the dispersion model whilst the gas separator was modeled as a completely mixed tank. All parameters needed for the model were obtained from independent experiments both carried out in this work and reported elsewhere. Simulation results were compared with a number of experimental data obtained from the systems with various geometrical and operational conditions. It was shown that the model could predict the oxygen mass transfer between phases in the ALC with reasonable accuracy.

Keywords: Airlift contactor (ALC), dispersion model, mass transfer, mathematical model, *and* verification.

INTRODUCTION

Airlift contactors (ALCs) have become attractive to many biotechnological applications due to their several advantages over the conventional bioreactors (Chisti and Moo-Young 1987). One of the most important factors in the operation of such ALCs is the rate of gas–liquid mass transfer which controls the uptake and removal of low soluble components such as oxygen and carbon dioxide.

Extensive effort has been paid to investigate the mass transfer characteristics of ALCs and these were reviewed by Chisti (1998), and Merchuk and Gluz (1999). Empirical correlations for the estimation of the overall mass transfer coefficient, $K_L a$, were available according to various geometries and operating conditions of the contactor. This parameter is important for the development of mathematical model for the ALC as it provides information on the rate at which mass transfer takes place through the gas–liquid interface.

Several mathematical models for mass transfer in the ALC have been proposed where many of them were simplified by neglecting the kinetics of mass transfer between gas and liquid in the various sections of the system (Camarasa et al. 2001, Choi 1999, Dhaouadi et al. 1997, Dhaouadi et al. 2001, Lindert et al. 1992). In external loop airlift

contactors, the interaction between gas and liquid in the downcomer may be neglected without interrupting the predicting capability of the model because there exists very little, if not none, depending on the gas flow rate and the geometry of the connection between riser and downcomer, amount of gas in this section. However, this situation is unlikely for internal loop ALCs where a large fraction of gas holdup is usually present in all of the sections of the system including downcomer. Mathematical models for the internal loop ALC were usually more complicated and subjected to parameter fittings with experimental data (Korpijarvi et al. 1999). This, by and large, limits the use of the models to some specific experimental ranges.

This work intended to investigate the accuracy of the mass transfer model developed for the internal loop ALC. In the model development, the ALC was considered as three interconnecting sections where the interactions between gas and liquid in each section were taken into consideration. To ensure the general use of the model, parameter estimations were performed using independent experiments, and in many cases, they were obtained from other independent sources.

EXPERIMENTAL

Experimental apparatus

A schematic diagram of the experimental setup for this work is shown in Figure 1. Experiments were performed in an airlift contactor (ALC) made of a transparent acrylic cylindrical column. The column was 0.137 m. in diameter and 1.2 m. in height. The ratio between cross sectional areas of downcomer and riser (A_d/A_r) could be altered by changing the draft tube size. Detail on dimensions of draft tubes is provided in Table 1.

Table 1. Specification of ALCs Used

Draft tube diameter (m)		Sparger location	A_d/A_r (-)
Internal	External		
0.093	0.10	Annular	1
0.0735	0.079	Annular	0.43
0.034	0.04	Annular	0.067
0.093	0.10	Draft tube	1

In all experiments, air was distributed continuously via a gas sparger into the water-filled column. The gas sparger was constructed of 0.008 m diameter PVC-tube with an orifice diameter fixed at 0.001 m. The gas sparger could be located at the base of either annular or draft tube sections of the ALC. Detail on specifications of each contactor employed in this work is also given in Table 1. The unaerated liquid level was controlled at 3 cm above the top of the draft tube. Air flowrate was controlled by a calibrated rotameter to give 0.0059–0.0737 ms^{-1}. The column was equipped with pressure ports located 0.1 m apart along the contactor height. These ports could be connected to a water manometer for pressure drop measurement and also employed as tracer injection points for the determination of liquid velocities in the ALC.

The overall gas holdup was determined by the volume expansion method whereas the gas holdup in the annulus section of the system could be estimated using the reading from the manometer where

$$\varepsilon_{G,An} = 1 - \frac{\Delta P_{manometer}}{\rho_L g \Delta h} \qquad (1)$$

Gas holdup from Eq. (1) was a *riser gas holdup* if gas was sparged in the annulus section of the ALC and a *downcomer gas holdup* if gas was sparged in the draft tube. It was assumed further that the gas holdup in the top section was approximately equal to that in the riser. This allowed the estimation of the downcomer gas holdup as one could perform simple calculation where the overall gas holdup was equal to the sum of the gas holdups in riser, gas separator and downcomer (equation not shown here).

Liquid velocity was measured using the color tracer technique. The color tracer was injected into the ALC and the time between two fixed points along the height of the column was measured and employed in the calculation of liquid velocity:

$$v_L = \frac{L}{t} \qquad (2)$$

The overall volumetric mass transfer coefficient ($K_L a$) was determined by the dynamic

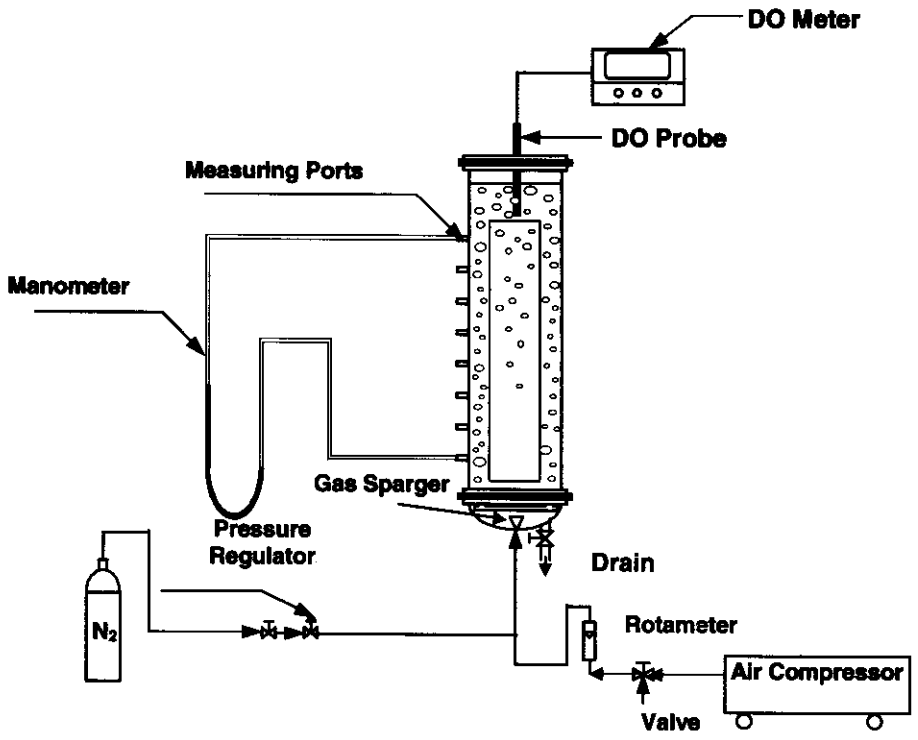

Figure 1. Schematic Diagram of Experimental Setup

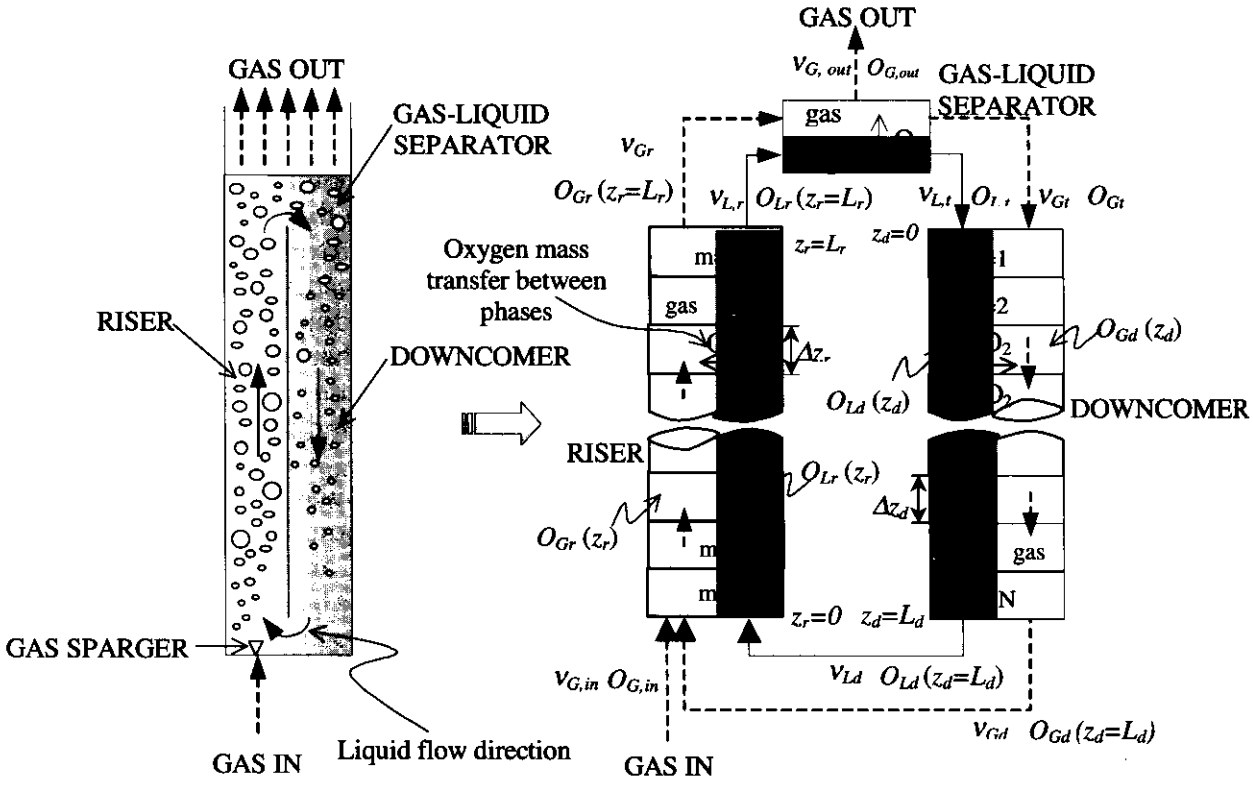

Figure 2. Block Flow Representation of the Internal Loop ALC

method (Koide et al. 1983b, Tung et al. 1998, Bouaifi et al. 2001). A dissolved oxygen meter (Jenway 9300) was used to record the time profile of O_2 concentration in the ALC that was freed of O_2 by bubbling N_2 through for approximately 30 min. K_La was then determined from the slope of the plot between $\ln\left(\frac{O_{Gi}^{*}-O_{Li}}{O_{Gi}^{*}-O_{L}}\right)$ and t.

MATHEMATICAL MODEL DEVELOPMENT

The ALC was assumed to consist of three main sections as shown in the schematic diagram in Figure 2. The first section is the "riser" to which the gas is supplied. A mixture of gas and liquid moved from the riser to the "gas separator" located at the top of the contactor. A large fraction of gas bubbles disengaged from the system here while the liquid and the remaining portion of small bubbles moved further to the "downcomer." In this last section, no gas supply was provided and the fluid content moved downwards and re-entered the riser at the bottom of the column together with the inlet gas. To construct a mathematical model for this system, each part of the ALC was considered separately as illustrated in the right side of Figure 2. The riser and downcomer were represented by the dispersion model with the exchange of oxygen between gas and liquid phases in each volume element. No liquid was added or removed from the system, whereas gas entered the system only at the bottom section of the riser and left the contactor at the gas separator. The behavior of the gas separator was assumed to be well mixed. Hence, the overall model is represented by a series of various types of reactors, which is the *dispersion-stirred tank-dispersion.*

For simplicity, the model was developed by considering the following assumptions:

1. The effect of hydrostatic head on solubility of oxygen is negligible. This is reasonable for small-scale systems.
2. The overall volumetric mass transfer coefficient is uniform.
3. The gas holdup is uniform within each individual region.

Following the mass conservation principal, the following set of equations was obtained.

Gas-phase oxygen concentration in the riser and downcomer:

at 0<zi<Li:

$$\frac{\partial}{\partial t}O_{Gi}(z_i)=-v_{Gi}\frac{\partial}{\partial z_i}O_{Gi}(z_i)+D_{Gi}\frac{\partial^2}{\partial z_i^2}O_{Gi}(z_i)-\frac{(1-\varepsilon_{Gi})}{\varepsilon_{Gi}}K_La\left(O_{Gi}(z_i)-HO_{Li}(z_i)\right) \quad (3)$$

Liquid-phase oxygen concentration in the riser and downcomer:

at 0<zi<Li:

$$\frac{\partial}{\partial t}O_{Li}(z_r)=-v_{Li}\frac{\partial}{\partial z_r}O_{Li}(z_i)+D_{Li}\frac{\partial^2}{\partial z_i^2}O_{Li}(z_i)+K_La\left(\frac{O_{Gi}(z_i)}{H}-O_{Li}(z_i)\right) \quad (4)$$

where $i = r$ for riser and $i = d$ for downcomer, H the Henry's law constant.

Gas-phase oxygen concentration in the gas separator:

$$\frac{d}{dt}O_{Gi}=\frac{\varepsilon_{Gr}A_rv_{Gr}O_{Gr}(z_r=L_r)-\varepsilon_{Gd}A_dv_{Gd}O_{Gd}(z_d=0)-Q_{Gout}O_{Gi}}{\varepsilon_{Gi}V_t}-\left(\frac{1-\varepsilon_{Gi}}{\varepsilon_{Gi}}\right)K_La(O_{Gi}-HO_{Li}) \quad (5)$$

Liquid-phase oxygen concentration in the gas separator:

$$\frac{d}{dt}O_{Ll} = \frac{(1-\varepsilon_{Gr})A_r v_{Lr} O_{Lr}(z_r = L_r) - (1-\varepsilon_{Gd})A_d v_{Ld} O_{Ld}(z_d = 0)}{(1-\varepsilon_{Gl})V_l} + K_L a\left(\frac{O_{Gl}}{H} - O_{Ll}\right) \qquad (6)$$

Boundary and initial conditions for this set of equations are given in Table 2, Eqs. (7) to (16). To ensure the accuracy of the simulation results, various numerical techniques were employed as equation solvers, which include the Crank-Nicholson, Forward Finite Difference, and the 4th order Runge-Kutta integration method (Chapra and Canale 1998). The simulation results were verified further with experimental findings as explained later on.

PARAMETER ESTIMATIONS

The model required that various hydrodynamic and mass transfer parameters be known a priori. These parameters were gas holdups (ε_r), liquid velocities (v_L), gas velocities (v_G), dispersion coefficients (D), and overall volumetric gas–liquid mass transfer coefficient, $K_L a$. These parameters were obtained from individual experiments as described previously. Experiments carried out in this work allowed the establishment of empirical correlations for the estimation of hydrodynamic and mass transfer parameters, as indicated in Table 3, Eqs. (17) to (21). It was noted that there was a limitation on the experiments on the draft tube sparged ALC; hence, the hydrodynamic and mass transfer parameters for this case were estimated from available empirical correlations. In this work, the reported correlations of Koide et al. (1983a) were used for predicting ε_{Go} and $K_L a$, whereas the correlations of Korpijarvi et al. (1999) were used for predicting ε_{Gr} and ε_{Gd}. Riser superficial liquid velocity, $v_{L,r}$, was predicted by the correlation of Chisti et al. (1988). These employed correlations are summarized in Table 4, Eqs. (22) to (26).

Other parameters could subsequently be calculated by using the following equations. Firstly, the downcomer liquid velocity, v_{Ld}, was calculated using the continuity equation:

$$v_{Lr} A_r (1-\varepsilon_{Gr}) = v_{Ld} A_d (1-\varepsilon_{Gd}) \qquad (27)$$

Table 2. Initial and Boundary Conditions in Each Section of the ALC

				Eq'ns.
Riser	*I.C.*	Gas	$O_{Gr}(0 \le z_r \le L_r,\ t=0) = 0$	(7)
	B.C.		$O_{Gr}(z_r = 0,\ t>0) = \left(\frac{v_{Gd} A_d O_{Gd}(z_r = 0,\ t>0) + Q_{G,in} O_{G,in}}{v_{Gr} A_r}\right)$	(8)
	I.C.	Liquid	$O_{Lr}(0 \le z_r \le L_r,\ t=0) = 0$	(9)
	B.C.		$O_{Lr}(z_r = 0,\ t>0) = O_{Ld}(z_d = L_d,\ t>0)$	(10)
Downcomer	*I.C.*	Gas	$O_{Gd}(0 \le z_d \le L_d,\ t=0) = 0$	(11)
	B.C.		$O_{Gd}(z_d = 0,\ t>0) = O_{Gl}(t>0)$	(12)
	I.C.	Liquid	$O_{Ld}(0 \le z_d \le L_d,\ t=0) = 0$	(13)
	B.C.		$O_{Ld}(z_d = 0,\ t>0) = O_{Ll}(t>0)$	(14)
Gas–Liquid Separator	*I.C.*	Gas	$O_{Ll}(t=0) = 0$	(15)
	I.C.	Liquid	$O_{Gl}(t=0) = 0$	(16)

I.C. – Initial Condition *B.C. – Boundary Condition*

Table 3. Empirical Correlations Used for Predicting Hydrodynamic and Mass Transfer Behavior in Annulus Sparged ALCs

Correlation	Eq'ns
$K_L a = 0.288\left(A_d/A_r\right)^{-0.17} u_{sg}^{0.74}$	(17)
$\varepsilon_{Gr} = 1.267\left(A_d/A_r\right)^{-0.25} u_{sg}^{0.93}$	(18)
$\varepsilon_{Gr} = 1.306\left(A_d/A_r\right)^{-0.21} u_{sg}^{0.92}$	(19)
$\varepsilon_{Gd} = 0.865\varepsilon_{Gr} - 0.0038$	(20)
$v_{Lr} = 0.241 + 0.604\left(A_d/A_r\right)^{1.14} u_{sg}^{0.324}$	(21)

where the riser liquid velocities, v_{Lr}, in the annulus sparged and draught tube sparged ALCs were estimated from Eqs. (21) and (26), respectively. Riser gas velocity, v_{Gr}, was calculated from v_{Lr} and slip velocity in the riser, v_{sr}, as follows:

$$v_{Gr} = v_{Lr} + v_{sr} \tag{28}$$

In general, v_{sr} is a function of the terminal rise velocity of a single bubble, v_r, where the hindering effects from neighboring bubbles in the riser was taken into account. Literature showed that v_{sr} did not vary much with conditions in the ALC, and it was assumed here to be constant at 0.25 ms^{-1} (Merchuk and Stein 1981).

Downcomer gas velocity, v_{Gd}, was, in a similar fashion, calculated using the continuity equation.

$$v_{Gd} = \frac{v_{Gr} A_r \varepsilon_{Gr} - Q_{G,in}}{A_d \varepsilon_{Gd}} \tag{29}$$

At this point, axial dispersion coefficients in gas and liquid phases both in riser and downcomer (D_{Gr}, D_{Gd}, D_{Lr}, and D_{Ld}) remained still unknown. The reported values of these parameters from literature were, therefore, assimilated to the model directly without manipulation. The liquid phase dispersion coefficients (D_{Lr} and D_{Ld}) were reported by several investigators (Merchuk et al. 1998, Moustiri et al. 2001) where it was shown that these parameters were in the range of 0.002–0.02 m^2s^{-1} at μ_{Sg} between 0.01 and 0.1 ms^{-1}. Gas phase dispersion coefficients (D_{Gr} and D_{Gd}) were reported (Magnartz and Pilhofer 1981, Rüffer et al. 1994) to be 2–5 m^2s^{-1} for the ALC at μ_{Sg} between 0.01–0.1 ms^{-1}. Hence, the values of D_{Gr}, D_{Gd}, D_{Lr}, D_{Ld} used in all simulations were selected arbitrarily from these ranges as 3, 1, 0.01, and 0.01 m^2s^{-1}, respectively.

RESULTS AND DISCUSSION

Accuracy of model prediction

To verify the ability of the model in predicting oxygen mass transfer behavior between gas and liquid phases in the internal loop ALC, the simulation results were compared with experimental data both from this work and elsewhere. Details of all design and operating conditions of the employed experimental works are provided in Table 5. Our preliminary results

Table 4. Empirical Correlations Used for Predicting Hydrodynamic and Mass Transfer Behavior in Draft Tube Sparged ALCs

Correlation	Eq'ns	References
$\frac{\varepsilon_{Gas}}{(1-\varepsilon_{Gas})^4} = 0.124\left(\frac{u_{sg}\mu}{\sigma}\right)^{0.966}\left(\frac{\rho\sigma^3}{g\mu^4}\right)^{0.294}\left(\frac{D_i}{D_o}\right)^{0.114}$ for water-air system $\frac{k_L a D_o^2}{D_{O_2}} = 0.477\left(\frac{\mu}{\rho D_{O_2}}\right)^{0.5}\left(\frac{gD_o^2\rho}{\sigma}\right)^{0.873}\left(\frac{gD_o^3\rho^2}{\mu^2}\right)^{0.257}\left(\frac{D_i}{D_o}\right)^{-0.542}\varepsilon_{Gas}^{1.36}$	(22) (23)	Koide *et al.* (1983a)
$\varepsilon_{Gr} = 0.67u_{sg}^{0.57}$ for $A_d/A_r = 0.59$ $\varepsilon_{Gr} = 0.85u_{sg}^{0.66}$ for $A_d/A_r = 1.22$ $\varepsilon_{Gr} = 0.77u_{sg}^{0.66}$ for $A_d/A_r = 2.70$ $\varepsilon_{Gr} = 0.65u_{sg}^{0.75}$ for $A_d/A_r = 7.14$ $\varepsilon_{Gd} = 0.84\varepsilon_{Gr}$	(24) (25)	Korpijarvi *et al.* (1999)
$v_{Lr}(1-\varepsilon_{Gr}) = \left(\frac{2gH_D(\varepsilon_{Gr}-\varepsilon_{Gd})(1-\varepsilon_{Gd})^2}{11.402(A_d/A_h)^{0.789}(A_r/A_d)^2}\right)^{0.5}$	(26)	Chisti *et al.* (1988)

Table 5. Design and Operating Parameters for the Experiments Reported in Literature

Ref. No.	Source	H_{dl} (m)	A_d/A_r (-)	u_{sg} (ms^{-1})	Sparger Location
W11	This work	1	0.067	0.01	Annular
W12		1	0.067	0.07	
W13		1	0.067	0.12	
B11	Bello *et al.* (1985)	1.45	0.56	0.01	
K11	Koide *et al.* (1983a)	0.7	0.54	0.01	
K21		1.4	0.54	0.01	
K31		2.1	0.54	0.01	
K41		1.4	1.327	0.01	
W21	This work	1	1	0.023	Draft tube
W22		1	1	0.04	
W23		1	1	0.06	
W24		1	1	0.08	
K51	Koide *et al.* (1983b)	1.4	0.69	0.03	
K61		1.4	1.39	0.03	
K71		1.4	3.31	0.03	
K81		0.7	1.76	0.03	
K91		1.4	1.76	0.03	
K82		0.7	1.76	0.08	
K92		1.4	1.76	0.08	

showed that the several numerical techniques employed to solve the mathematical model provided similar sets of results indicating that the model predictions were accurate and consistent. The results presented thereafter in this article were limited to those obtained from the 4th order Runge-Kutta integration method, and the reported oxygen concentration is in dimensionless form.

Experimental verification of the mathematical model

For annulus sparged ALCs, Eqs. (17)–(21) were used in estimating the hydrodynamic and mass transfer parameters in the model. Figure 3 illustrates the comparisons between the simulation results and experimental data on liquid phase oxygen concentration in the riser, O_{Lr}, in the system at different superficial gas velocities, u_{sg}. In general, both simulation results and experimental data demonstrated that the oxygen concentration profile reached equilibrium concentration more rapidly with increasing u_{sg}. It can be seen that the model produced results with a reasonable accuracy when compared with experimental data for all range of u_{sg} (0.01–0.12 ms^{-1}).

The model was further verified by comparing the results at various ratios between downcomer and riser cross-sectional areas, A_d/A_r. Both experimental results from the present work and

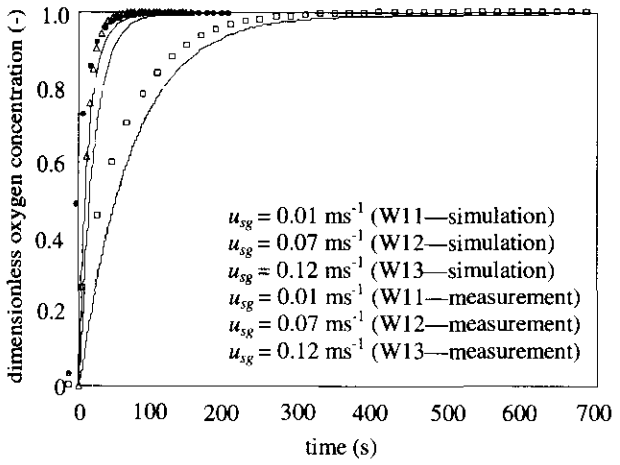

Figure 3. Comparison of Simulation Results and Experimental Data of Time Profiles of $O_{L,r}$ in Annulus Sparged ALCs Experimental Data at A_d/A_r=0.067

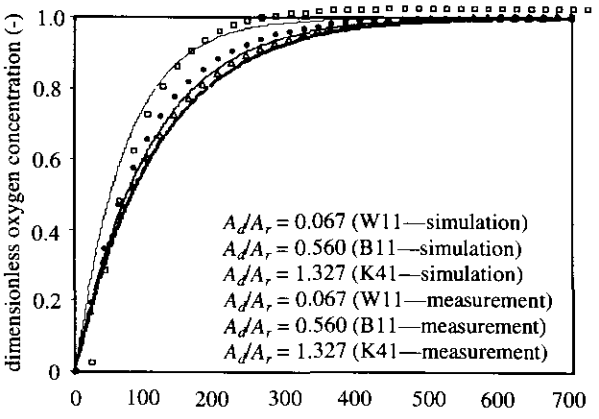

Figure 4. Comparison of Simulation Results and Measurement of Time Profiles of $O_{L,r}$ in Annulus Sparged ALCs: Effect of A_d/A_r

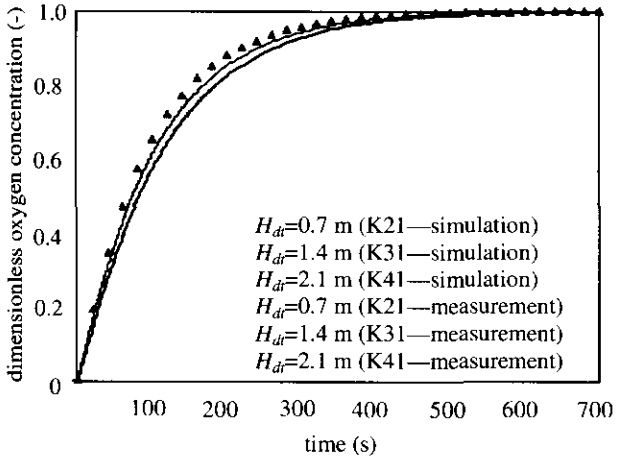

Figure 5. Comparison of Simulation Results and Measurement of Time Profiles of $O_{L,r}$ in Annulus Sparged ALCs: Effect of H_{dt}

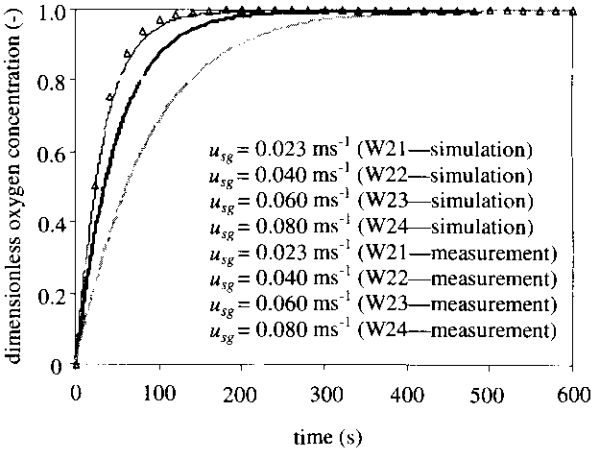

Figure 6 . Comparison of Simulation Results and Measurement of Time Profiles of $O_{L,r}$ in Draft Tube Sparged ALCs: Effect of u_{sg}

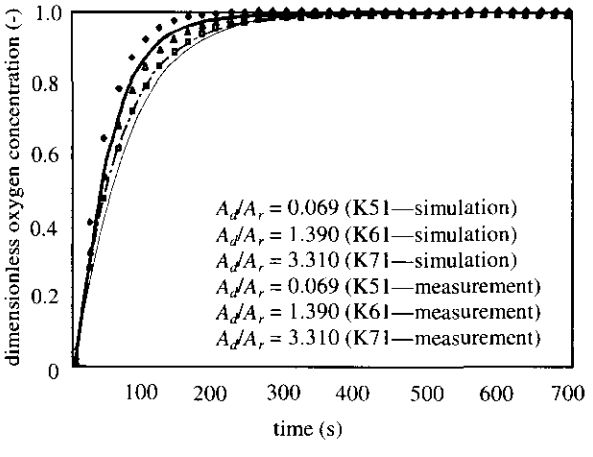

Figure 7. Comparison of Simulation Results and Measurement of Time Profiles of $O_{L,r}$ in Draft Tube Sparged ALCs: Effect of A_d/A_r

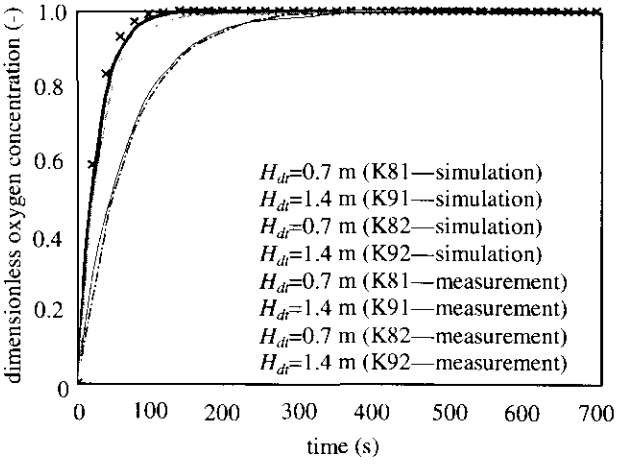

Figure 8. Comparison of Simulation Results and Measurement of Time Profiles of $O_{L,r}$ in Draft Tube Sparged ALCs: Effect of H_{dt}

from literature were used in this comparison as demonstrated in Figure 4. The oxygen concentration profile was found to reach equilibrium more quickly when A_d/A_r decreased. These results were consistent with the data reported by other researchers (Koide et al. 1983a, 1983b, Chisti and Moo-Young 1987, Korpijarvi et al. 1999).

Figure 5 depicts the comparison between the simulation results and experimental data on O_{Lr} at different draft tube heights, H_{dt}. The simulation was found to agree well with the reported experiment (Koide et al. 1983b) which indicated that H_{dt} had negligible effect on transient liquid phase oxygen concentration.

To further verify the validity of the model, experimental data in the draft tube sparged ALC presented in this work and those reported by Koide et al. (1983a) were also compared with the simulation results. In this case, Eqs. (17)–(21) were no longer appropriate due to differences in hydrodynamic and mass transfer behavior in the annulus sparged and draft tube sparged ALCs. These equations were, therefore, substituted by the reported empirical correlations for the draft tube sparged ALC, Eqs. (22)–(26).

Figures 6–8 show a comparison between experimental data and simulation results on O_{Lr} in the draft tube sparged ALC at different u_{sg}, A_d/A_r and H_{dt}, respectively. The results indicate a good agreement between simulation and experiment.

CONCLUSIONS

In brief, the developed model was found to be reasonably accurate in predicting the mass transfer behavior in the internal loop airlift contactor (ALC) without the need of parameter fittings. This shows that the airlift contactor can well be represented by a series of models where the riser and downcomer are represented by the dispersion model and the gas separator by the completely mixed tank.

This knowledge is significant for further application of this mathematical model in the systems with more complicated interaction between various chemical species such as reactions. The reaction term can just simply be added to the right side of the equation to account for the reaction taking place in the airlift reactor.

ACKNOWLEDGMENTS

The authors wish to acknowledge the Thailand Research Fund for the financial support.

NOTATIONS

A	cross-sectional area, m^2
D	dispersion coefficient, $m^2 s^{-1}$
D_i	inside diameter, m
D_o	outside diameter, m
g	gravitational acceleration, $m^2 s^{-1}$
H	Henry constant, $kgmol\ m^{-3}\ gas/kgmol\ m^{-3}\ liquid$
H_D	dispersion height, m
H_{dt}	draft tube height, m
$K_L a$	overall mass transfer coefficient, s^{-1}
L	length, m
O	oxygen concentration, $kg\ m^{-3}$
O^*	equilibrium oxygen concentration, $kg\ m^{-3}$
Q	volumetric flowrate, $m^3\ s^{-1}$
t	time, s
u	superficial velocity, $m\ s^{-1}$
u_∞	terminal rise velocity, $m\ s^{-1}$
u_{sg}	superficial gas velocity, $m\ s^{-1}$
v	velocity, m
v_s	slip velocity, m
z	axial distance, m
Δh	distance between pressure measurement points, m
$\Delta P_{manometer}$	hydrostatic pressure difference between two measuring points, Pa
ε	holdup, -
μ	viscosity, $kg\ m^{-1}\ s^{-1}$
ρ	density, $kg\ m^{-3}$
σ	surface tension, $N\ m^{-2}$

Subscripts

b	bottom
d	downcomer
G	gas phase

o	overall
r	riser
t	top
in	input
out	output
an	annulus

REFERENCES

Bouaifi, M., Hebrard, G., Bastoul, D., and Roustan, M. (2001). "A comparative study of gas hold-up, bubble size, interfacial area and mass transfer coefficients in stirred gas–liquid reactors and bubble columns," *Chem. Eng. Proc., 40,* 97–111.

Camarasa, E., Meleiro, L. A. C., Carvalho, E., Domingues, A., Fiho, R. M., Wild, G., Poncin, S., Midoux, N., and Bouillard, J. (2001). "A complete model for oxidation air-lift reactors," *Comp. Chem. Eng., 25,* 577–584.

Chapra, S. C., and Canale, R. P. (1998). *Numerical methods for engineers with programming and software applications,* 3rd ed., McGraw-Hill, New York.

Chisti, Y. (1998). "Pneumatically agitated bioreactors in industrial and environmental bioprocessing: Hydrodynamics," *Appl. Mech. Rev., 51,* 33–112.

Chisti, Y., and Moo-Young, M. (1987). "Airlift reactors: Characteristics, applications and design considerations," *Chem. Eng. Commun., 60,* 195–242.

Chisti, M. Y., Halard, B., and Moo-Young, M. (1988). "Liquid circulation in airlift reactors," *Chem. Eng. Sci., 43,* 451–457.

Choi, K. H. (1999). "A mathematical model for unsteady-state oxygen transfer in an external-loop airlift reactor," *Korean. Chem. Eng., 16,* 441–448.

Dhaouadi, H., Poncin, S., Hornut, J. M., Wild, G., Oinas, P., and Korpijarvi, J. (1997). "Mass transfer in an external-loop airlift reactor: Experiments and modeling," *Chem. Eng. Sci., 52,* 3909–3917.

Dhaouadi, H., Poncin, S., Midoux, N., and Wild, G. (2001). "Gas–liquid mass transfer in an airlift reactor—Analytical solution and experimental confirmation," *Chem. Eng. Proc., 40,* 129–133.

Koide, K., Kurematsu, K., Iwamoto, S., Iwata, Y., and Horibe, K. (1983a). "Gas holdup and volumetric liquid-phase mass transfer coefficient in bubble column with draught tube and with gas dispersion into tube," *J. Chem. Eng. Japan, 16,* 413–419.

Koide, K., Sato, H., and Iwamoto, W. (1983b). "Gas holdup and volumetric liquid-phase mass transfer coefficient in bubble column with draught tube and with gas dispersion into annulus," *J. Chem. Eng. Japan, 16,* 407–413.

Korpijarvi, J., Oinas, P., and Reunanen, J. (1999). "Hydrodynamics and mass transfer in an airlift reactor," *Chem. Eng. Sci., 54,* 2255–2262.

Lindert, M., Kochbeck, B., Prüss, J., Warnecke, H.-J., and Hempel, D.C. (1992). "Scale-up of airlift-loop bioreactors based on modeling the oxygen mass transfer," *Chem. Eng. Sci., 47,* 2281–2286.

Mangartz, K.-H., and Pilhofer, T. H. (1981). "Interpretation of mass transfer measurements in bubble columns considering dispersion of both phases," *Chem. Eng. Sci., 36,* 1069–1077.

Merchuk, J. C., and Gluz, M. (1999). "Bioreactors, airlift reactors," Flickinger, M.C. and Drew, S.W., eds., *Encycolpedia of bioprocess technology: Fermentation, biocatalysis and bioseparation,* vol. 1, Wiley, New York, 320–353.

Merchuk, J. C., and Stein, Y. (1981). "Local hold up and liquid velocity in airlift reactors," *AIChE J., 27,* 377–388.

Merchuk, J. C., Contreras, A., Garcia, F., and Molina, E. (1998). "Studies of mixing in a concentric tube airlift bioreactor with different spargers," *Chem. Eng. Sci., 53,* 709–719.

Moustiri, S., Hebrard, G., Thakre, S. S., and Roustan, M. (2001). "A unified correlation for predicting liquid axial dispersion coefficient in bubble columns," *Chem. Eng. Sci., 56,* 1041–1047.

Rüffer, H. M., Liwei Wan, Lübbert, A., and Schügerl, K. (1994). "Interpretation of gas residence time distributions in large airlift tower loop reactors," *Bioproc. Eng., 11,* 153–159.

Tung, H.-L., Tu, C.-C., Chang, Y.-Y., and Wu, W.-T. (1998). "Bubble characteristics and mass transfer in an airlift reactor with multiple net draft tubes," *Bioproc. Eng.*, *18*, 323–328.